Nanoscale Research Letters

NANO EXPRESS Open Access

Electrochemical Reduction of CO_2 on Hollow Cubic Cu_2O@Au Nanocomposites

Wei Tan[1,2], Bo Cao[1], Wenqiu Xiao[1], Min Zhang[1], Shoushan Wang[1], Shilei Xie[1], Dong Xie[1], Faliang Cheng[1*], Qingquan Guo[2*] and Peng Liu[1*]

Abstract

Surfactant-free and low Au loading Cu_2O@Au and Au hollow cubes, based on electrodeposited Cu_2O cubes as sacrificed templates, were prepared by means of a galvanic replacement reaction (GRR). The electrocatalytical performance of the as-prepared catalysts towards carbon dioxide (CO_2) electrochemical reduction was evaluated. The experimental results show that Cu_2O@Au catalyst can convert CO_2 to carbon monoxide (CO) with a maximum Faradaic efficiency (FE) of ~ 30.1% at the potential of − 1.0 V (vs. RHE) and is about twice the FE of the other catalysts at the same potential. By comparison, such electrocatalytical enhancement is attributed to the metal-oxide interface in Cu_2O@Au.

Keywords: CO_2 electrochemical reduction, Cuprous oxide, Hollow cubes, Metal-oxide interface

Background

CO_2 is considered as the main greenhouse gas that contributes to global warming; therefore, finding an effective way to convert/store CO_2 has attracted more and more attention [1, 2]. The main methods for reducing CO_2 concentration in the atmosphere include CO_2 capturing and storing it underground [3, 4] or convert it to added value chemicals [5–7]. Due to the stable chemical properties of CO_2, it is necessary to use high temperature, high pressure, or catalyst to make it reactive. Considering the energy and economy cost, electrochemical conversion of CO_2 under mild conditions is a promising strategy for decreasing the excess greenhouse gas and achieving an artificial carbon cycle [8–10]. However, the major difficulties in CO_2 electrochemical reduction are the intrinsic stability of CO_2, the lower potential of CO_2 reduction reaction (CO_2RR), and the low selectivity for reduction products [11]. Thus, it is urgent to develop CO_2 reduction catalysts with high selectivity, good stability, and excellent activity.

Previous studies show several metallic electrodes, such as Au, Ag, Cu, Pd, and Sn, are attractive candidates for CO_2RR [12]. Among them, copper is the only metal catalyst which is found to produce considerable C1–C3 hydrocarbon products and alcohols [13]. Au, which is a highly active catalyst towards CO_2 electrochemical reduction, can produce CO from CO_2 with high selectivity and low overpotential [11]. Except for Cu and Au, the other metal electrodes including Ag, Pd, and Sn primarily convert CO_2 to CO or formate ($HCOO^-$) via a two-electron transfer pathway [14–17]. However, on the one hand, it is difficult to improve the selectivity and stability of Cu-based catalysts towards the electrochemical reduction of CO_2 to C1–C3 hydrocarbon products. On the other hand, Au is highly selective for CO production, but its high cost and rare-earth abundance hinder its industrialization in CO_2RR [18, 19]. The composites based on copper and gold are of great potential for CO_2 electrochemical reduction. But most of the currently reported CuAu catalysts were synthesized via solvothermal method [20]. The morphology of the nanoparticles is difficult to control, and these particles tend to be easily oxidized and aggregated [21, 22]. Therefore, it is very important to develop a kind of gold and copper composite with controllable morphology, high stability, and high product selectivity for CO_2 electrochemical reduction. Besides, it is reported that the metal-oxide interface could improve the electrocatalytical activity of the catalysts towards CO_2RR [23].

* Correspondence: liupeng@dgut.edu.cn; chengfl@dgut.edu.cn; qqg55555@163.com
[1]Guangdong Engineering and Technology Research Center for Advanced Nanomaterials, School of Environment and Civil Engineering, Dongguan University of Technology, Dongguan 523808, China
[2]School of Chemical Engineering and Light Industry, Guangdong University of Technology, Guangzhou 510006, China

Here in this paper, we report a surfactant-free Cu_2O@Au nanocomposite in which Cu_2O/Au interface was constructed for electrocatalytical reduction of CO_2 in water. For comparison, the hollow cubic Au catalysts were prepared by dissolving Cu_2O in Cu_2O@Au catalysts in ammonia. The experimental results showed that the metal/oxide interface in Cu_2O@Au catalyst could activate inert CO_2 molecule and increase the FE of CO. The CO FE is 30.1% on Cu_2O@Au electrode at − 1.0 V (vs. RHE) which is twice than that on Cu_2O and Au electrodes prepared in this work. This result not only proved the metal-oxide interface could improve the electrocatalytical activity of the electrodes towards CO_2RR, but also paved the way for metal-oxide catalyst synthesis.

Methods

Materials

Copper (II) trifluoroacetate (Cu $(TFA)_2$, 98%), potassium trifluoroacetate (KTFA, 98%), and chloroauric acid ($HAuCl_4$, 99.9%) were purchased from Sigma-Aldrich and used directly without any purification. All solutions were prepared with Milli-Q ultrapure water (Millipore ≥ 18.2 MΩ cm). Nitrogen (N_2) (99.999%) and CO_2 (99.999%) gases used in the experiment were purchased from Foshan MS Messer Gas CO., Ltd. Carbon paper which thickness is 0.3 mm was purchased from Hesen in Shanghai.

Preparation of Cu_2O Nanocubes and Cu_2O@Au

Cu_2O nanocubes were synthetized according to the method reported in previous literature [24]. The cubic Cu_2O nanoparticles were electrodeposited on a carbon paper (1 cm × 1 cm) using chronoamperometry at − 0.06 V (vs. SCE) for 1 h in 10 mM Cu $(TFA)_2$ and 0.2 M KTFA solution. Before the Cu_2O nanocubes electrodeposition, the carbon paper was washed by water and ethanol several times.

The preparation of Cu_2O@Au composite was immersing Cu_2O cubes into 2 mL $HAuCl_4$ (1 mM) solution for 30 min at 277 K.

Preparation of Hollow Cubic Au

The as-prepared Cu_2O@Au composite was immersed in 2 M ammonia water for 12 h at 277 K to remove Cu_2O and retain hollow cubic Au on the carbon paper.

Characterization

The morphologies and structures of nanomaterials were characterized by scanning electron microscopy (SEM, JEOL-6701F) equipped with an energy dispersive X-ray (EDX) detector system. The X-ray diffraction (XRD) patterns were recorded using Rigaku Ultima IV X-ray diffractometer with Cu Kα radiation (λ = 1.5406 Å) to study the compositions of the products.

Electrochemical Measurements of CO_2

Electrochemical measurements were carried out with a CH Instruments 760D (Chenhua, Shanghai) and a three-electrode system. The CO_2 electrochemical reduction was carried out in a two-compartment H-type cell with an Ag/AgCl and a platinum sheet (1 cm × 1 cm) used as reference and counter electrodes, respectively. Compensation for 85% iR drop was used in CO_2 electrochemical reduction. In this work, all potentials reported in the CO_2 electrochemical reduction were referenced against the reversible hydrogen electrode (RHE). The RHE used the following conversion: E_{RHE} (V) = $E_{Ag/AgCl}$ (V) + 0.197 V + (0.059 V × pH) [25]. A diagrammatic sketch of the H-type electrochemical cell is shown in Fig. 1. The two electrochemical cells were separated by a proton exchange membrane (Nafion 117, Sigma-Aldrich).

Linear sweep voltammetry (LSV) experiments were performed in 0.1 M $KHCO_3$ solution under N_2 (99.999%) or CO_2 (99.999%) atmosphere. Prior to LSV tests, N_2 or CO_2 were purged into the solution in H-type electrochemical cell for 20 min, respectively.

Before CO_2RR experiments, the electrolyte solution was saturated for 20 min with CO_2 and the pH of the 0.1 M $KHCO_3$ solution was about 8.6. The CO_2 electrochemical reduction was performed under potentiostatic conditions while the current and product concentration were monitored. The as-prepared materials were used as working electrodes. The CO_2RR experiments were repeated thrice at each potential. Detection of CO_2 reduction products were used by an online gas chromatography (GC Agilent, 7890B). A GC run was conducted every 930 s. The GC was equipped with two Plot-Q columns, a thermal conductivity detector (TCD), a flame ionization detector (FID), and a demethanizer with N_2 (99.999%) as carrier gas. The contents of liquid products were neglected in this work. During the CO_2RR experiments, CO_2 was vented into the cathode electrolysis cell at a flow rate of 20 ml min^{-1} continuously.

$$i_x = \frac{C_x \cdot q \cdot p}{RT} \cdot n_x F \tag{1}$$

$$\mathrm{FE}(\%) = \frac{i_x}{i_{total}} \cdot 100 \tag{2}$$

The FE calculation equation is shown in Eqs. 1 and 2, in which i_{total} is the current density recorded by the potentiostat during CO_2RR [26]. The partial current (i_x) which is needed to generate each product (x = H_2, CO, CH_4, C_2H_4) is derived from Eq. 1. C_x is extracted from the calibration curve GC volume concentration of product x. n_x is the number of reduced electrons required to produce x from carbon dioxide molecules. q is the gas flow rate, p is constant pressure, and T is the

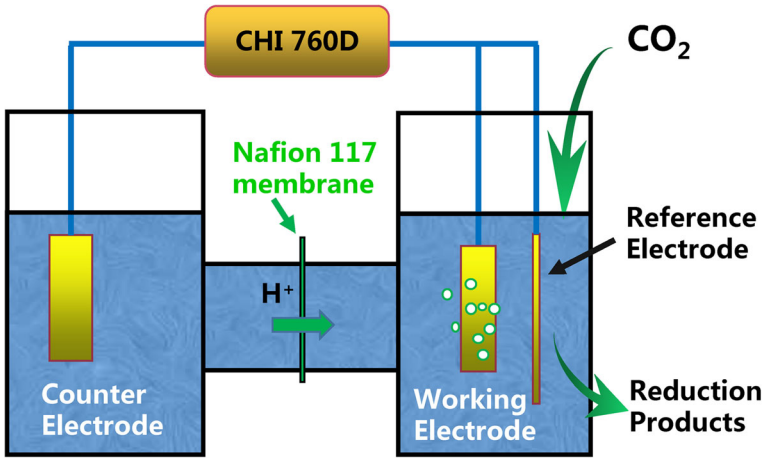

Fig. 1 A diagrammatic sketch of the H-type electrochemical cell

room temperature. *R* is the gas constant, and *F* is the Faradaic constant.

Results and Discussion

Morphology

The morphologies and structures of as-prepared Cu_2O and Cu_2O@Au nanocubes characterized by SEM were shown in Fig. 2. The Cu_2O nanocubes electrodeposited on the carbon paper had regular shapes and smooth surface (Fig. 2a). The average edge length of the Cu_2O cubes was about 1 μm as shown in Fig. 2b. An appropriate reaction time and Au^{3+} solution concentration of GRR on Cu_2O nanoparticles would produce Cu_2O@Au nanostructures as shown in Fig. 2c and d.

After Cu_2O nanocubes were immersed in $HAuCl_4$ (1 mM) solution for 30 min, the surface distribution of Au and Cu of Cu_2O@Au composites was examined by EDX mapping shown in Fig. 2e and f. It showed that Au nanoparticles were

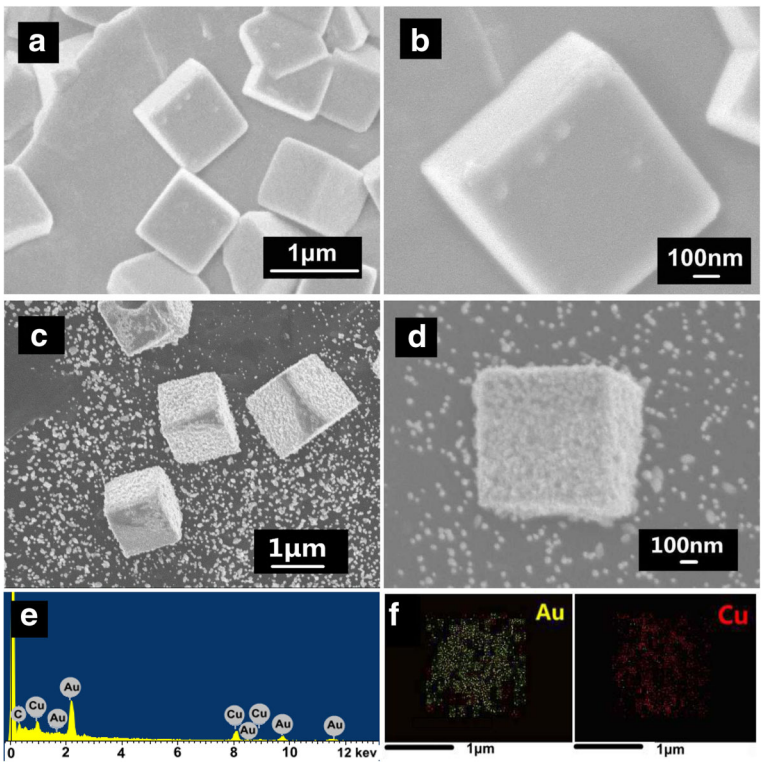

Fig. 2 The SEM images of Cu_2O nanocubes (**a**, **b**), Cu_2O@Au nanoparticles (**c**, **d**), and EDX of Cu_2O@Au nanoparticles (**e**, **f**)

uniformly distributed on the Cu_2O nanocube surface. The GRR between Cu_2O and $HAuCl_4$ involves the evolution of an internal hollow core and surface precipitation of Au nanoparticles [27, 28].

As shown in Fig. 3, Cu_2O in Cu_2O@Au composites was removed and the retained Au nanoparticles inherit the cubic frame of the Cu_2O@Au composites, after Cu_2O@Au nanocubes were immersed in ammonia water for 12 h. The small Au nanoparticles in hollow cubic Au framework were about 20~30 nm in diameter.

XRD Analysis

The crystal structure of the as-prepared catalysts was investigated by XRD, and the diffraction patterns were shown in Fig. 4. The diffraction peak at $2\theta = 54.51°$ belongs to the carbon paper. The diffraction peaks at $2\theta = 36.46$, 42.36, 61.44, and 73.55° are ascribed to the (111), (200), (220), and (311), respectively, of the Cu_2O cube (JCPDS 78-2076). Four weak peaks at $2\theta = 38.18$, 44.39, 64.57, and 77.54° are assigned to the (111), (200), (220) and (311), respectively, of Au (JCPDS 04-0784) which replaced Cu_2O on the carbon paper. Most of Cu_2O were substituted by Au; thus, the diffraction peaks corresponded to Cu_2O disappeared in XRD pattern of hollow cubic Au.

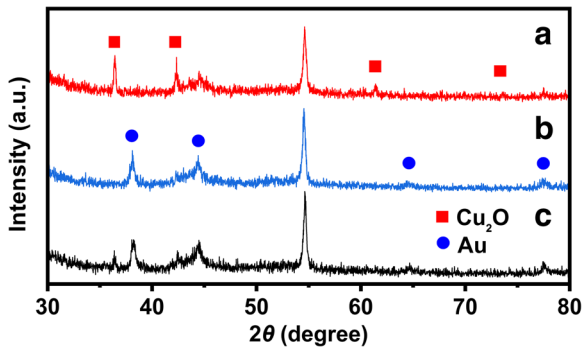

Fig. 4 XRD patterns of (a) Cu_2O cube, (b) hollow cubic Au, and (c) Cu_2O@Au

CO_2 Electrochemical Reduction Performance

The LSV curves of Cu_2O cube, Cu_2O@Au, and hollow cubic Au electrodes are shown in Fig. 5. The LSV experimental condition was obtained at a cathodic sweeping rate of 50 mV s^{-1} with N_2-saturated or CO_2-saturated 0.1 M $KHCO_3$ solution. The current density of all the three samples under the N_2 atmosphere is higher than that under CO_2; this difference may be caused by the hydrogen evolution reaction (HER) on Cu_2O cube, Cu_2O@Au, and hollow cubic Au, i.e., with continuous flow of CO_2 in the cathodic electrolytic cell, the surface of the electrode is covered by adsorbed CO molecules which will inhibit the HER on electrode surface and decrease the reduction current [29]. The current density of Cu_2O@Au electrode in CO_2-saturated 0.1 M $KHCO_3$ solution is higher than Cu_2O and hollow cubic Au electrodes as shown in Fig. 5d.

The electrochemistry method of amperometric *i–t* was used to evaluate the performance of CO_2RR in 0.1 M $KHCO_3$ solution at room temperature under atmospheric pressure. The potentials are set between − 0.7 and − 1.2 V for subsequent product determination. At different potentials, the FE of H_2 and CO for CO_2RR on Cu_2O cubes have a significant difference, as shown in Fig. 6a, i.e., the FE of H_2 is decreasing because the surface of Cu_2O cubes is covered by CO molecules produced by CO_2RR, and the HER is inhibited [30]. The FE of CH_4 and C_2H_4 vary slightly in different potentials.

The FE of Cu_2O@Au catalyst is shown in Fig. 6b. The FE of CO keeps upward trend with potential decreasing and reaches a maximum of 30.1%, at − 1.0 V (vs. RHE). The FE of H_2 decreases from 56.7 to 45.6%. Compared with the Cu_2O@Au catalyst, the maximum CO FE of hollow cubic Au catalyst is 16.3% at − 1.0 V (Fig. 6c). The CO FE of Cu_2O@Au catalyst at − 1.0 V is about twice of hollow cubic Au catalyst at the same potential. Cu_2O@Au composite shows superior catalytic activity for CO_2 electrochemical reduction than Cu_2O cube catalyst and hollow cubic Au catalyst, and it is related to the interfacial effect of metal oxides.

To understand the reaction mechanism on CO_2RR to CO, we considered the following reaction steps:

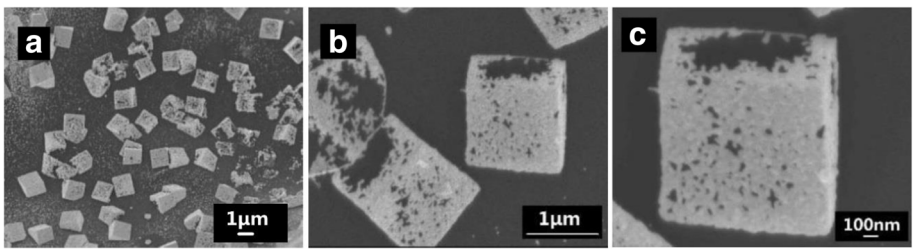

Fig. 3 The SEM images of hollow cubic Au (**a**–**c**) of different magnification

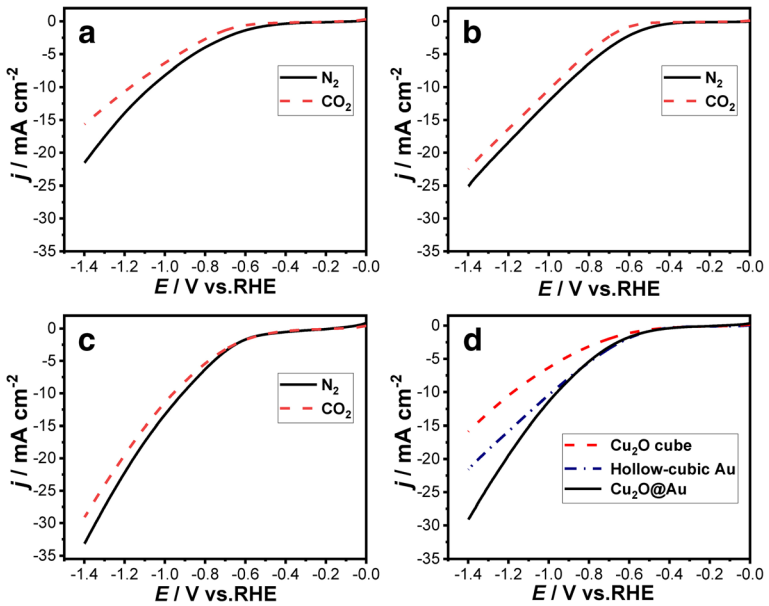

Fig. 5 LSV curves obtained on **a** Cu_2O cube, **b** hollow cubic Au, and **c** Cu_2O@Au electrodes in N_2-saturated (black solid line) and CO_2-saturated (red dotted line) 0.1 M $KHCO_3$ solutions. **d** LSV curves of the three samples in CO_2-purged 0.1 M $KHCO_3$ solutions

$$CO_2(g) + * + H^+(aq) + e^- \rightarrow {}^*COOH \quad (3)$$

$${}^*COOH + H^+(aq) + e^- \rightarrow {}^*CO + H_2O(l) \quad (4)$$

$${}^*CO \rightarrow CO(g) + * \quad (5)$$

Generally, Eq. 3 is perceived as the potential limiting step on CO_2RR to CO [23]. The corresponding binding energy can be substantially lowered on the interface of Cu_2O@Au, compared to the Cu_2O cube surface or Au surface. In addition, the Eq. 4 and Eq. 5 are also facilitated at the Cu_2O@Au interface. It indicates that the interfacial effect of metal oxides could enhance the CO_2 adsorption and the electrochemical surface area [31, 32]. The Cu_2O@Au catalyst consists of Cu_2O and Au

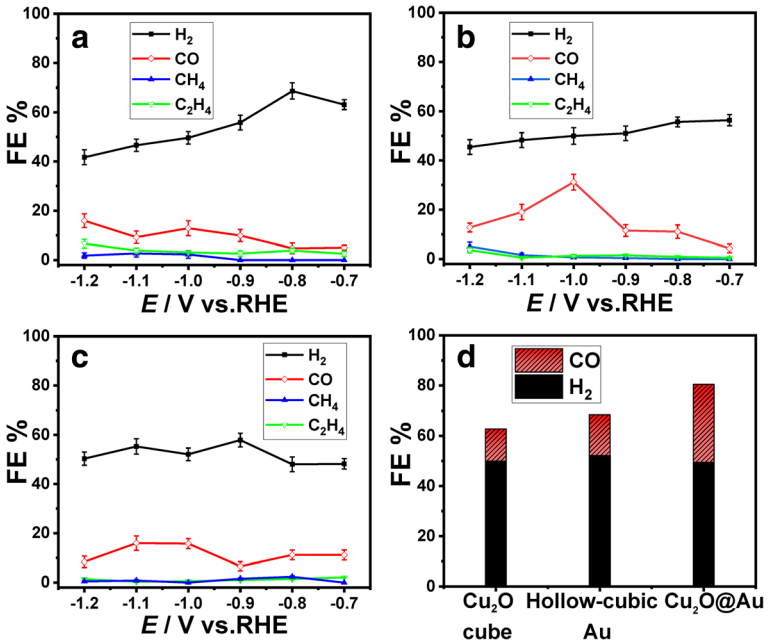

Fig. 6 FE of **a** Cu_2O cube catalyst, **b** Cu_2O@Au catalyst, and **c** hollow cubic Au catalyst. **d** Comparison of FE for CO and H_2 at − 1.0 V vs RHE on three catalysts

nanoparticles can supply a metal-oxide interface to activate inert CO_2 molecules, enhance charge transfer efficiency, and increase FE of CO [33].

Compared to the mass transfer effect of hollow cubic Au catalyst composed by Au nanoparticles, the synergistic interactions of metal oxides fabricated by Cu_2O cubes and Au nanoparticles are more advantageous to convert CO_2 into CO by CO_2 electrochemical reduction.

The FE comparison for CO and H_2 at − 1.0 V vs RHE on Cu_2O cube catalyst, Cu_2O@Au catalyst, and hollow cubic Au catalyst is shown in Fig. 6d. The H_2/CO ratio of these three catalysts is as follows: 3.9, 3.2, and 1.7. The Cu_2O@Au catalyst production ratio of 1.7 by CO_2 electrochemical reduction is closest to that of syngas (the mixture of CO and H_2) ratio of 2 [34, 35]. The catalyst surface construct method and the proportion of product gases would contribute to design highly selective CO_2RR catalysts.

The average current density of three catalysts, which were performed by amperometric *i*–*t*, is shown in Fig. 7. With the potential increase, it shows evidently increasing current densities of three catalysts as expected. The difference of the average total current density between hollow cubic Au (blue solid line) and Cu_2O@Au (black solid line) expands at − 1.0 V. However, the difference of the average total current density between hollow cubic Au and Cu_2O cube (red solid line) is not marked within − 0.7 to − 1.1 V. Consequently, we could conclude that the charge transfer efficiency of Cu_2O@Au catalyst is higher than the other two catalysts.

Conclusions

In summary, surfactant-free and low Au loading electrodes for CO_2 electrochemical reduction were prepared by electrodeposition and GRR. The Cu_2O@Au catalyst shows superior catalytic activity for CO_2RR than Cu_2O cubes and hollow cubic Au catalyst due to the metal-oxide interface, i.e., the metal-oxide interface could activate the inert CO_2 molecules absorbed on electrodes. For Cu_2O@Au catalyst, it can convert CO_2 to CO with a maximum FE of ~ 30.1% at − 1.0 V and is about twice of the other catalysts at the same potential. The produced gas of Cu_2O@Au catalyst by CO_2 electrochemical reduction has a H_2/CO ratio of 1.7, which is close to the syngas ratio of Fischer–Tropsch process of 2. Based on these results, we can draw some conclusions that the Cu_2O@Au catalyst fabricated by Cu_2O cubes and Au nanoparticles could form a metal/oxide interface to activate inert CO_2 molecules and this catalyst could be applied to syngas production by CO_2 electrochemical reduction.

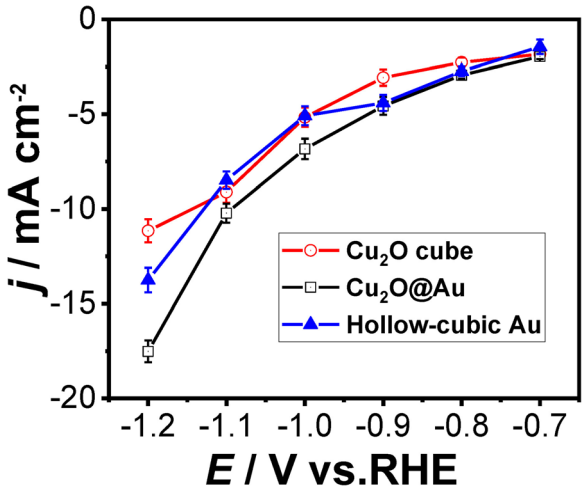

Fig. 7 The average total current density of the three catalysts for CO_2 reduction at different potentials

Abbreviations

CO: Carbon monoxide; CO_2: Carbon dioxide; CO_2RR: CO_2 reduction reaction; EDX: Energy dispersive X-ray; GC: Gas chromatography; GRR: Galvanic replacement reaction; $HCOO^-$: Formate; HER: Hydrogen evolution reaction; LSV: Linear sweep voltammetry; N_2: Nitrogen; RHE: Reversible hydrogen electrode; SEM: Scanning electron microscopy; XRD: X-ray diffraction

Acknowledgements

This work was supported by the National Natural Science Foundation of China (No. 21505019, 21775022, 21701054, 51878169), Natural Science Foundations of Guangdong Province (No.2017A030310603), and Guangdong Provincial Key Platform and Major Scientific Research Projects for Colleges and Universities (No. 2015KCXTD029, 2016KTSCX135, 2016KCXTD023, 2017KQNCX196).

Availability of Data and Materials

All data are fully available without restriction.

Authors' Contributions

PL and FC designed the experiments. WT, BC, and WX carried out the experiments. WT prepared the manuscript. SW, DX, and XS analyzed the XRD and SEM data. QG and MZ analyzed the electrochemistry data. All authors read and approved the final manuscript.

Ethics Approval and Consent to Participate

We declare that there are no concerning data of human and animals.

Competing Interests

The authors declare that they have no competing interests.

Publisher's Note

Received: 5 December 2018 Accepted: 4 February 2019
Published online: 21 February 2019

References

1. Graves CR, Ebbesen SD, Mogensen M, Lackner KS (2011) Sustainable hydrocarbon fuels by recycling CO_2 and H_2O with renewable or nuclear energy. Renew Sust Energ Rev 15(1):1–23
2. Ganesh I (2014) Conversion of carbon dioxide into methanol – a potential liquid fuel: fundamental challenges and opportunities (a review). Renew Sust Energ Rev 31(2):221–257
3. Whipple DT, Kenis PJA (2010) Prospects of CO_2 utilization via direct heterogeneous electrochemical reduction. J Phys Chem Lett 1(24): 3451–3458
4. Yang H, Xu Z, Fan M, Gupta R, Slimane RB, Bland AE (2008) Progress in carbon dioxide separation and capture: a review. J Environ Sci 20(1):14–27

5. Appel AM, Bercaw JE, Bocarsly AB, Dobbek H, DuBois DL, Dupuis M (2013) Frontiers, opportunities, and challenges in biochemical and chemical catalysis of CO_2 fixation. Chem Soc Rev 113(8):6621–6658
6. Olah GA, Prakash GK, Goeppert A (2011) Anthropogenic chemical carbon cycle for a sustainable future. J Am Chem Soc 133(33):12881–12898
7. Costentin C, Robert M, Savéant JM (2013) Catalysis of the electrochemical reduction of carbon dioxide. Chem Soc Rev 42(6):2423–2436
8. Huang Y, Handoko AD, Hirunsit P, Yeo BS (2017) Electrochemical reduction of CO_2 using copper single-crystal surfaces: effects of CO* coverage on the selective formation of ethylene. ACS Catal 7:1749–1756
9. Liu S, Tao H, Zeng L, Liu Q, Xu Z (2017) Shape-dependent electrocatalyticreduction of CO_2 to CO on triangular silver nanoplates. J Am Chem Soc 139(6):2160–2163
10. Ogura K (2013) Electrochemical reduction of carbon dioxide to ethylene: mechanistic approach. J CO2 Util 1:43–49
11. Zhao S, Tang Z, Guo S, Han M, Zhu C (2017) Enhanced activity for CO_2 electroreduction on a highly active and stable ternary Au-CDots-C_3N_4 electrocatalyst. ACS Catal 8(1):188–197
12. Bagger A, Ju W, Varela AS, Strasser P, Rossmeisl J (2017) Electrochemical CO_2 reduction: a classification problem. Chemphyschem 18(22):3266–3273
13. Hori Y (2008) Electrochemical CO_2 reduction on metal electrodes. In: Modern Aspects of Electrochemistry. Springer New York, New York City, pp 89–189
14. Wu J, Ma S, Sun J, Gold J, Tiwary CS (2016) A metal-free electrocatalyst for carbon dioxide reduction to multi-carbon hydrocarbons and oxygenates. Nat Commun 7:13869
15. Hori Y, Wakebe H, Tsukamoto T, Koga O (1994) Electrocatalytic process of CO selectivity in electrochemical reduction of CO_2 at metal electrodes in aqueous media. Electrochim Acta 39(11–12):1833–1839
16. Xie JF, Huang YX, Li WW, Song XN, Xiong L (2014) Efficient electrochemical CO_2 reduction on a unique chrysanthemum-like Cu nanoflower electrode and direct observation of carbon deposite. Electrochim Acta 139(26):137–144
17. Qiao J, Liu Y, Hong F, Zhang J (2014) A review of catalysts for the electroreduction of carbon dioxide to produce low-carbon fuels. Chem Soc Rev 43:631–675
18. Wang XL, Varela AS, Bergmann A, Kühl S, Strasser P (2017) Catalyst particle density controls hydrocarbon product selectivity in CO_2 electroreduction on CuO_x. Chemsuschem 10(22):4642–4649
19. Ham YS, Kim MJ, Choi J, Choe S, Lim T (2016) Fabrication of Au catalysts for electrochemical reduction of CO_2 to syngas. J Nanosci Nanotechnol 16(10): 10846–10852
20. Kim D, Resasco J, Yu Y, Asiri AM, Yang P (2014) Synergistic geometric and electronic effects for electrochemical reduction of carbon dioxide using gold-copper bimetallic nanoparticles. Nat Commun 5:4948
21. Christophe J, Doneux T, Buess-Herman C (2012) Electroreduction of carbon dioxide on copper-based electrodes: activity of copper single crystals and copper-gold alloys. Electrocatalysis 3(2):139–146
22. Andrews E, Fang Y, Flake J (2018) Electrochemical reduction of CO_2 at CuAu nanoparticles: size and alloy effects. J Appl Electrochem 148:435–441
23. Gao DF, Zhang Y, Zhou ZW, Cai F, Zhao XF, Huang WG, Li YS, Zhu JF, Liu P, Yang F, Wang GX, Bao XH (2017) Enhancing CO_2 electroreduction with the metal-oxide interface. J Am Chem Soc 139(16):5652–5655
24. Liu P, Cheng ZY, Ma L, Qiu YF, Chen MQ, Cheng FL (2016) Cuprous oxide template synthesis of hollow-cubic Cu_2O@PdxRuy nanoparticles for ethanol electrooxidation in alkaline media. RSC Adv 6:76684–76690
25. Ren D, Deng Y, Handoko AD, Chen CS, Malkhandi S (2015) Selective electrochemical reduction of carbon dioxide to ethylene and ethanol on copper (I) oxide catalysts. ACS Catal 5(5):2814–2821
26. Lee SY, Jung H, Kim NK, Oh HS, Min BK (2018) Mixed copper states in anodized Cu electrocatalyst for stable and selective ethylene production from CO_2 reduction. J Am Chem Soc 140:8681–8689
27. Xiong L, Li SW, Zhang B, Miao P, Du YC, Miao P, Han YX, Zhao HT, Xu P (2015) Galvanic replacement-mediated synthesis of hollow Cu_2O-Au nanocomposites and Au nanocages for catalytic and SERS applications. RSC Adv 5(93):76101–76106
28. Xia XH, Wang Y, Ruditskiy A, Xia YN (2013) 25th anniversary article: galvanic replacement: a simple and versatile route to hollow nanostructures with tunable and well-controlled properties. Adv Mater 25(44):6313–6333
29. Kim D, Lee S, Ocon JD, Jeong B, Lee JK (2014) Insights into an autonomously formed oxygen-evacuated Cu_2O electrode for the selective production of C_2H_4 from CO_2. Phys Chem Chem Phys 17(2):824–830
30. Lee S, Park G, Lee J (2017) The importance of Ag-Cu biphasic boundaries for selective electrochemical reduction of CO_2 to ethanol. ACS Catal 7(12): 8594–8604
31. Wang YF, Han P, Lv XM, Zhang LJ, Zheng GF (2018) Defect and interface engineering for aqueous electrocatalytic CO_2 reduction. Joule 2(12):2551–2582
32. Chu S, Ou P, Ghamari P, Vanka S, Zhou B (2018) Photoelectrochemical CO_2 reduction into syngas with the metal/oxide interface. J Am Chem Soc 140(25):7869–7877
33. Zhang WY, Qin Q, Dai L, Qin RX, Zhao XJ, Chen XM, Ou DH, Chuong TT, Wu BH, Zheng FN (2018) Electrochemical reduction of carbon dioxide to methanol on hierarchical Pd/SnO_2 nanosheets with abundant Pd-O-Sn interfaces. Angew Chem Int Edit 57(30):9475–9479
34. Hernandez S, Farkhondehfal MA, Sastre F, Makkee M, Saracco G (2017) Syngas production from electrochemical reduction of CO_2: current status and prospective implementation. Green Chem 19(10):2326–2346
35. Hoffman ZB, Gray TS, Moraveck KB, Gunnoe TB, Zangari G (2017) The electrochemical reduction of carbon dioxide to syngas and formate at dendritic copper-indium electrocatalysts. ACS Catal 7(8):5381–5390